
Simulating large emitters using CMAQ and a local scale finite element model. Analysis of the surroundings of Barcelona

Albert Oliver*

University Institute for Intelligent Systems and
Numerical Applications in Engineering (SIANI),
University of Las Palmas de Gran Canaria (ULPGC),
Campus de Tafira, 35017, Las Palmas de Gran Canaria, Spain
Email: albert.oliver@ulpgc.es

*Corresponding author

Raúl Arasa

Technical Department,
Meteosim S.L.,
Barcelona Science Park,
Baldiri Reixac 10-12, 08028, Barcelona, Spain
Email: rarasa@meteosim.com

Agustí Pérez-Foguet

Barcelona School of Civil Engineering,
Department of Civil and Environmental Engineering,
University Research Institute for
Sustainability Science and Technology,
Universitat Politècnica de Catalunya – BarcelonaTech (UPC),
Jordi Girona 1-3, 08034 Barcelona, Spain
Email: agusti.perez@upc.edu

M^a Ángeles González

Technical Department,
Meteosim S.L.,
Barcelona Science Park,
Baldiri Reixac 10-12, 08028, Barcelona, Spain
Email: magonzalez@meteosim.com

Abstract: In this work, we present a novel approach to simulate large emitters in the microscale. The main idea is to combine a nested grid approach and a finite element model to simulate the subgrid scale. The nested grid system consists of the mesoscale meteorological model WRF-ARW, the Air Emission Model of Meteosim (AEMM), and the air quality model CMAQ. The subgrid scale is simulated using an adaptive, Eulerian, non-steady finite element model. The results from the nested grid simulation are used as initial and boundary

conditions in the subgrid model, making this approach one-way. A simulation has been carried out in the surroundings of Barcelona, where an important contributor to the sulphur dioxide levels is considered. The simulations were carried out for one episode with high levels of sulphur dioxide. The time period of the simulation was 48 hours with a 24-hour spin-up.

Keywords: air quality modelling; subgrid scale plume modelling; nested grid modelling; plume-in-grid; microscale; plume rise; weather research and forecasting model; Air Emission Model of Meteosim; community multi-scale air quality; finite element method.

Reference to this paper should be made as follows: Oliver, A., Arasa, R., Pérez-Foguet, A. and González, M.Á. (xxxx) 'Simulating large emitters using CMAQ and a local scale finite element model. Analysis of the surroundings of Barcelona', *Int. J. Environment and Pollution*, Vol. X, No. Y, pp.xxx-xxx.

Biographical notes: Albert Oliver received his PhD from the Universitat Politècnica de Catalunya and is currently a Postdoctoral Researcher at the University of Las Palmas de Gran Canaria. His research interest is the application of the finite element method in environmental problems, and particularly in the simulation of air quality and wind fields at the microscale level. He is also working on the generation of tetrahedral adapted meshes for these problems.

Raúl Arasa is the Project Director of Meteosim, where he leads the technical department. He holds a PhD in Physics and Master's in Meteorology. He has extensive experience in meteorology, air quality and atmospheric modelling. During his career, he has worked in the development, implementation and execution of coupled air quality modelling systems, adapting different meteorological and dispersion/photochemical models, and implementing emissions inventories and emissions models. He has been involved in monitoring systems and air quality assessment and he has contributed to the Emergency Plans and operational air quality modelling systems under current legislation.

Agusti Pérez-Foguet holds a PhD in Civil Engineering and works as a Professor at the Universitat Politècnica de Catalunya. His main research interests are in the field of numerical and statistical modelling applied to environmental engineering and sustainable development. He currently works in developing strategies for accurate simulation of air quality at the microscale level, and in the definition and implementation of decision support systems in the water and sanitation sector.

M^a Ángeles González works as the Project Manager at Meteosim. She previously worked on air quality modelling for five years in Centre for Energy, Environment and Technology (CIEMAT), where she researched air pollution and heavy metals with chemistry-transport models. She holds a PhD in Physics and Master's in Geophysics and Meteorology (from the Complutense Univ. of Madrid). She has experience in meteorological and air quality modelling systems and has participated in emission inventories development, numerous air quality modelling studies, the model execution, and subsequent processing, and data analysis and graphics.

This paper is a revised and expanded version of a paper entitled 'Simulating large emitters using CMAQ and a local scale finite element model. Analysis in the surroundings of Barcelona' presented at the 17th International Conference on Harmonisation within Atmospheric Dispersion Modelling for Regulatory Purposes, Budapest, Hungary, 9–12 May 2016.

1 Introduction

Air quality is an environmental issue that directly affects much of the population, causing 2.4 million deaths annually, according to estimates from the World Health Organization (EEA, 2007). Thus, it is of vital importance to study the impact of air quality, especially in urban areas. However, mesoscale air quality models are not sensitive enough to calculate the concentrations on the local scale that affect health. In the case of large emitters, the problem in Eulerian mesoscale models resides in the size of the grid. The pollutants emitted are instantaneously diffused in the computational cell. For this reason, efforts have been made to simulate the subgrid scale using different techniques (Karamchandani et al., 2011). The most commonly used approaches are the nested grid, plume-in-grid (PinG), and hybrid models. In this work, we propose a new addition to these methods based on the resolution of the transport and reaction of pollutants, using a mesh adapted to the terrain and the concentration. This approach includes the numerical solution of model equations with the finite element method (FEM). To illustrate the advantages and disadvantages of the proposal, we first describe the main characteristics of current approaches.

Nested grid modelling consists of using a finer grid in the region of interest. The method solves all scales involved in the problem using a set of nested grids. The global scale is solved with a coarse grid; in the region of interest of the continental scale, this grid is split horizontally by a factor of three, and this is repeated recursively for the smaller scales. Typical horizontal grid resolutions are 64 km, 32 km, 16 km, 8 km, and 4 km for the different scales. The approach is known as one-way nesting when the larger scale results are used to set the boundary and initial conditions for the smaller scales. When the results of the nested model are also used in the larger scale, it is called two-way nesting. The US Environmental Protection Agency (EPA) models-3/community multi-scale air quality (CMAQ) model (Byun and Schere, 2006) use this technique to simulate the different scales. This model usually uses a one-way approach and has been applied successfully to model air quality (Sokhi et al., 2006; Qin et al., 2015). Another model that uses both one-way and two-way nested grids is the Weather Research and Forecasting/Chemistry (WRF/Chem) model (Grell et al., 2005), which has been used in several applications (Žabkar et al., 2015; Wałaszek et al., 2015; Gao et al., 2016). The problem with the nested grid approach is that, since it uses a regular grid, the whole domain has to be refined using the same size, and once the domain is chosen, it cannot be changed dynamically. Note that although parallel versions of computational models reduce computational time, the spatial resolution and the size of domains of interest still make using the approach of uniform nested grids prohibitive.

The hybrid models combine the solution from a coarse grid model and the local scale. The variability of the solution is modelled at the local scale and computed offline. Knowing the variability allows a mesoscale simulation to be performed by adding the subgrid concentration. Several studies have been done to compute the variability (Marshall et al., 2008). Ching and Majeed (2012) have developed one approach to characterise the subgrid spatial variability on an hourly and grid-by-grid basis. The variability is studied using statistical methods and provided as probability density functions. Hybrid models are currently used for different purposes. The applications found in the literature usually consider local scales of the same extension as that covered by the coarse model; however, it should be noted that they model the phenomena involved in each scale in a distinct way. Hybrid models have been used to simulate the population exposure to hazardous air pollutants, e.g., using CMAQ and the hazardous air pollutant exposure model (HAPEM) (Rosenbaum, 2005), to predict the exposure estimates (Isakov et al., 2007, 2009), and to simulate the apportionment of pollutants from traffic (Cavellin et al., 2016). One of the advantages of this method is that the variability using simulated or measured data can be studied offline, and that this variability can then be used for the predictions. While this method saves a lot of computational time, it has the drawback of considering that this precomputed variability does not change.

The PinG model uses a puff or plume model to simulate the processes that happen at the subgrid scale. The subgrid model simulates the processes until the variability in the subgrid scale is no longer important, and then returns the solution to the grid model (Karamchandani et al., 2002). Thus, this technique is two-way. Most of the PinG models use Gaussian approximations for the plume trajectory. A plume model that has been developed specifically to simulate the subgrid phenomena is SCICHEM (Karamchandani et al., 2000; Chowdhury et al., 2015). The SCICHEM model incorporates complete gas, aqueous, and aerosol phases chemistry within the state-of-the-art Gaussian puff model second-order closure integrated puff (SCIPUFF). It can be coupled to CMAQ (Karamchandani et al., 2008, 2012, 2014) – it is referred to as CMAQ-APT (advanced plume treatment) – and has been employed successfully to characterise the impact of aircraft emissions in the Atlanta International airport (Rissman et al., 2013) and to simulate industrial emissions in the zone of Paris (Kim et al., 2014; Raffort et al., 2015). Currently, this approach is being incorporated into other mesoscale models besides CMAQ (Gressent et al., 2016; van der Swaluw et al., 2016) with encouraging results. This is a very promising approach to the problem, but the use of a Lagrangian approach has some drawbacks, such as collision with an obstacle or overlap of plumes when reactions are of interest. In this last situation, specific merging algorithms have to be used.

In this work, we propose another subgrid strategy that combines a nested grid model using CMAQ and an Eulerian subgrid scale dispersion model that uses the FEM. The FEM has been applied to air quality modelling (AQM) with good results (Liu and Leung, 2005; Albani et al., 2015). The nested grid simulation is an Eulerian coupled modelling system that uses the meteorological model WRF-ARW (Skamarock and Klemp, 2008; Skamarock et al., 2008), the emission model developed by Meteosim AEMM (Arasa et al., 2013, 2014, 2016a), and the US EPA models-3/CMAQ model. The subgrid scale is simulated using an adaptive, Eulerian, non-steady finite element model (Oliver et al., 2012, 2013). The results from the CMAQ simulation are used as boundary and initial conditions in the finite element model. This nesting is only one-way, so it can be used for

predictions in the domains of interest, but the results from the subgrid scale are not used for CMAQ forecasting. Therefore, both the CMAQ system and the local finite element model simulate air quality in the domain of interest, allowing both results to be compared. Note that emissions in the domain of interest of CMAQ are not inherited in the local scale model. A key advantage of the finite element model is that the tetrahedral mesh used to simulate the episode is adapted to the terrain, so that it only has small elements where it needs to, decreasing both the mesh size and the computational requirements. The first applications of the local scale finite element model have been presented with constant wind field conditions, and consequently with a single mesh for the overall simulation problem (Pérez-Foguet et al., 2006; Montenegro et al., 2012; Oliver et al., 2012). We previously proposed coupling a local model with mesoscale models by considering a set of meshes for simulating time evolution (Pérez-Foguet and Oliver, 2009). These meshes are fixed on an hourly basis in concordance with meteorological data. In this work, we include the latest developments of the local scale air quality model, including the dynamic adaptive strategy presented in Monforte and Pérez-Foguet (2013, 2014). This strategy allows capturing the evolution of the plume front using small elements, while the mesh is coarser in the zones in which the concentration is almost uniform. The local scale model can also be used to study the variability of the subgrid variables for its application in a hybrid method. It could also be an alternative to the current PinG plume model, with the Eulerian approach helping to overcome some of the drawbacks of the PinG method.

This paper presents an application of the new strategy applied to a large emitter located in the surroundings of Barcelona. Air quality measurement data have been provided by the Air Quality Network that belongs to the Territory and Sustainability Department of the Catalan Government. In the next section, we describe the area of study, the characteristics of the emitter and the episode, the stations used for validations, and a more detailed description of the models. In Section 3, we present and discuss the results obtained for both the WRF-ARW/AEMM/CMAQ model and the finite element model and compare them between themselves and against the observed data; and finally, in Section 4, we present the conclusions of this work.

2 Methodology

In this section, we present a description of the application. First, we specify the area of study, the location and characteristics of the emitter, and the network of stations; we then describe the modelling episode briefly; and finally, we develop in more detail the modelling system presented in this work.

2.1 Area of study

The area of interest is the surroundings of Barcelona. Barcelona is a large city on the Mediterranean coast of Spain located between two river mouths: the Besós river to the north, and the Llobregat river to the south. In the surroundings of Barcelona, and especially along the river basins, there are several industrial parks with large emitters. In the present work, we will study the emission of a large emitter of sulphur dioxide (SO₂) located in the Llobregat basin. In Figure 1, we show the simulation domains used by the

CMAQ modelling system. The CMAQ simulation has two nested domains. Figure 2 depicts a zoom of the CMAQ smaller domain, with the location of the emitter and the domain of the FEM shown. The domain of the finite element model is smaller than the CMAQ domain due to the computational cost. Looking at Figure 2, we can observe the basin of the Llobregat river that ends in a Delta, and the location of the emitter in the basin.

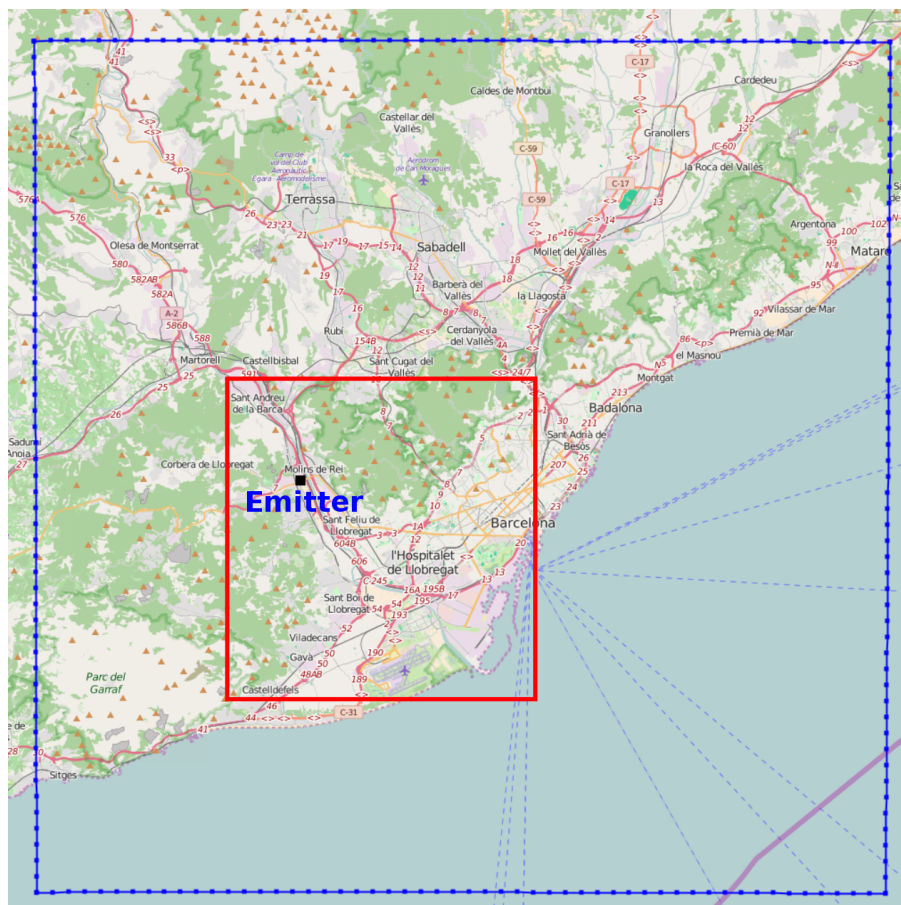
Figure 1 Nested domains of the WRF-ARW/AEMM/CMAQ modelling system (see online version for colours)



2.1.1 Emitter characteristics

The emitter is from a large industrial plant located in the Llobregat basin to the south-west of Barcelona, at position 416,442 m, 4,584,580 m (UTM 31N). The emitter is a stack with a height of 125 m and a diameter of 4.25 m. The SO₂ emission rate is 105 t/y with a gas output velocity of 10.33 m/s.

Figure 2 Finite element model domain, and location of the emitter (see online version for colours)



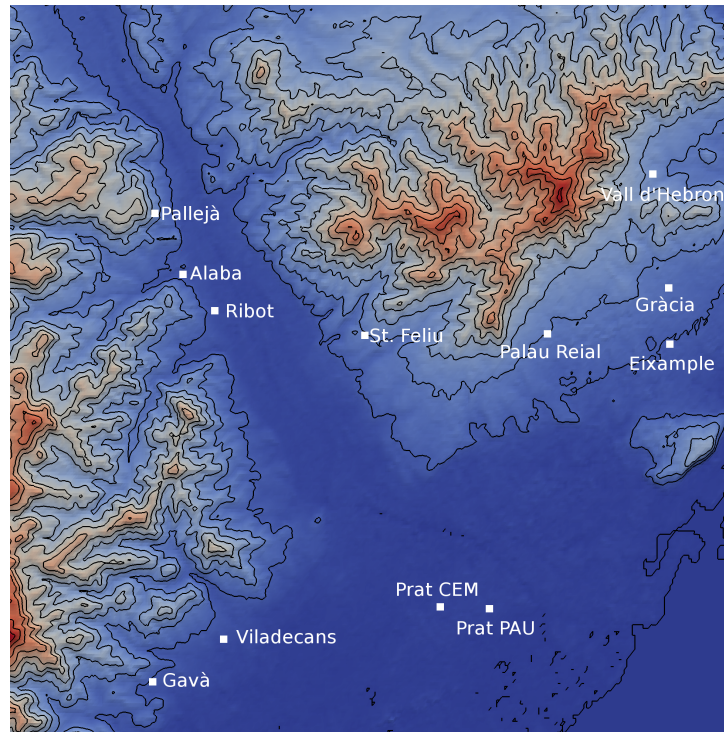
Note: The outer domain (blue) is the most inner CMAQ domain, and the red domain is the finite element model domain.

2.1.2 Validation stations

To validate the presented model, we used data from the Air Quality Network of the Catalan Government. The stations are located such that either urban or suburban areas are considered, with the source of the concentration from the background, the traffic, or industrial zones. Table 1 lists the name of the station, the coordinates, and the type of pollutants, while Figure 3 shows the locations of the stations marked on the domain of the local scale model. We want to remark that there are three stations near the large emitter: Alaba, Ribot, and Pallejà. All three of these stations will be used to validate our model, and we will use the Alaba station to do a more thorough analysis.

Table 1 Location of the measurement stations

<i>Name</i>	<i>XUTM (m)</i>	<i>YUTM (m)</i>	<i>Height (m)</i>	<i>Type</i>
Alaba	416,473	4,583,935	65	Suburban, industrial
Ribot	417,312	4,582,969	22	Suburban, industrial
Pallejà	415,730	4,585,559	82	Suburban, industrial
Gavà	415,669	4,573,101	25	Suburban, background
Viladecans	417,549	4,574,230	14	Suburban, traffic
St. Feliu	421,284	4,582,312	81	Suburban, industrial
Prat CEM	423,277	4,575,088	7	Suburban, traffic
Prat PAU	424,581	4,575,044	5	Suburban, traffic
Vall d'Hebron	428,902	4,586,612	129	Urban, background
Gràcia	429,323	4,583,573	75	Urban, traffic
Eixample	429,345	4,582,085	27	Urban, traffic
Palau Reial	426,114	4,582,355	81	Urban, traffic

Figure 3 Location of the measurement stations (see online version for colours)

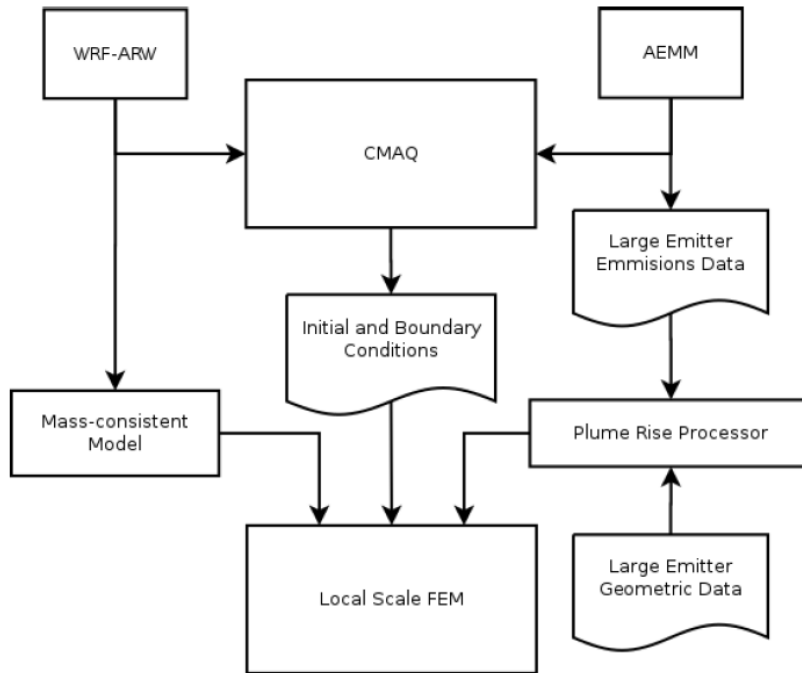
2.2 Modelling episode

The simulations were carried out on a day with a high concentration of SO₂ due to the atmospheric conditions. This criterion was selected to test the finite element model, to compare the results with the CMAQ system, and to determine its suitability for a high concentration day. The chosen day was 2 December 2013.

2.3 Modelling approach

Next, we outline the main feature of the two models presented in this work. Figure 4 represents the workflow of our approach. The modelling system consists of two different steps: a WRF-ARW/AEMM/CMAQ coupling system, and the local scale FEM. The WRF-ARW/AEMM/CMAQ system simulates the episode using a nested grid model up to a grid of 1 km. Its results are used for the local scale finite element model as boundary and initial conditions, while the meteorological data comes from WRF-ARW.

Figure 4 Workflow of the proposed methodology



Note: The first step (on top) is the WRFARW/AEMM/CMAQ modelling system, which is used for setting initial and boundary conditions in the local finite element model.

2.3.1 WRF-ARW/AEMM/CMAQ

We have used an Eulerian coupled modelling system (WRF-ARW/AEMM/CMAQ). The mesoscale meteorological model used is Weather Research and Forecasting-Advanced Research (WRF-ARW) version 3.6.1 (Skamarock and Klemp 2008), while the Air

Emission Model of Meteosim (AEMM v3.0) is a numerical, deterministic, Eulerian, local-scale model developed by Meteosim S.L. It allows the intensity of emissions in different areas, either anthropogenic (traffic, industry, residential, etc.) or natural (emissions caused by vegetation or erosion dust), to be obtained for the area of interest. Further, we used the US EPA models-3/CMAQ model to simulate the physical and chemical processes into the atmosphere. CMAQ is an open-source photochemical model that is updated periodically by the research community. In this contribution, we use CMAQ v5.0.1, considering CB-5 chemical mechanism and the associated Euler backwards iterative solver (Yarwood et al., 2005) and the AERO5 aerosol module (Carlton et al., 2010).

We ran a 48 hours numerical simulations for the selected day. A spin-up period of 24 hours was considered to minimise the influence of the initial conditions on the results. The WRF configuration follows the methodology defined in Arasa et al. (2016b); specifically, the initial and boundary conditions were taken from the NCEP/NCAR Climate Forecast System Reanalysis v2 (CFSv2) (Saha et al., 2014), using an spatial resolution of 0.5° and a temporal sampling of 6 hours. CFS represents the best state of the atmosphere since it incorporates satellite information, radio soundings, weather information from national services measurement stations, etc. CMAQ models could be initialised using models with coarse horizontal resolution corresponding to the global scale or using inner profiles. In this case, we used inner profiles, which are internal to the model and depend on the latitude. The vertical structure of the model includes 32 vertical layers.

2.3.2 *Finite element model*

The finite element model consists of a mesh generator, a wind mass-consistent model, and a plume-rise model; finally, the transport and reaction of pollutants is performed with a FEM stabilised with least squares. The model is coupled with the CMAQ system model in a one-way nesting, i.e., the results from the CMAQ system are used as boundary and initial conditions in the finite element model.

One of the advantages of using a FEM instead of a finite volume method is the capability to work with adapted meshes. The benefit of adapted meshes is that the number of elements needed to capture the geometry is smaller than using a regular grid. Specifically, we will generate a three-dimensional tetrahedral mesh adapted to the terrain.

Mesh construction will be carried out in two different steps. The first step is to create an adaptive triangular mesh of the terrain and all the desired vertical layers, and the second step is to generate the tetrahedral mesh. Usually, the terrain is given in the form of a uniform grid, e.g., a digital terrain model (DTM). The triangular mesh is adapted to the terrain using a formula proposed by Lee (2001) that relates the terrain curvature with the element size. Finally, a mesh adapted to the element sizes is constructed using a recursive decomposition of the geometry into quadrilaterals and finally obtaining triangles by splitting them (Sarrate and Huerta, 2000, 2001). Once the triangular meshes of the terrain and the inner layers are generated, a tetrahedral mesh adapted to the terrain is constructed using the Delaunay-based tetrahedral mesh generator Tetgen (Si, 2015).

The wind field is computed by interpolating the results from the WRF-ARW simulation and a mass-consistent model (Oliver et al., 2015). Once the wind field is computed, the plume rise has to be taken into account. Using the Briggs formulation, a three-dimensional trajectory of the plume is computed. This trajectory is modified to take

into account the atmospheric wind field, so that the final plume rise is a bent three-dimensional trajectory rather than contained in a plane. To force the pollutants to follow this trajectory during transport, the vertical component of the wind field obtained from the mass-consistent model is perturbed (Oliver et al., 2013). This is in contrast to the approximation followed by puff models, which focus on the Lagrangian description of the trajectory of discretised emissions.

Finally, the transport and reaction of the pollutants has to be simulated. The reactive term is highly nonlinear; for this reason, we apply an Strang splitting operator (Ropp et al., 2004), such that the transport and the reaction of the pollutants are solved independently. To solve transport, we use a FEM stabilised with least squares (Jiang, 1998). The stabilisation of the FEM is important to control the diffusion problems that arise with the classical Galerkin FEM. An advantage of the least squares FEM is that the resulting systems of equations are symmetric. These systems are solved with a conjugate gradient method preconditioned with an incomplete Cholesky factorisation density type (Lin and Moré, 1999; Rodríguez-Ferran and Sandoval, 2007). The chosen chemical mechanism is the same used by the CMAQ system – specifically, the carbon bond chemical mechanism CB05 and the Euler backward iterative (EBI) method – coupled with the finite element model to solve the chemical reactions.

In this work, a novel approach for the transport step is included. The first approaches for coupling scales simulated transport and reaction with fixed meshes, one for each wind field configuration given by the mesoscale, typically on an hourly basis (Pérez-Foguet and Oliver, 2009). The results at the end of one hour are projected into the mesh of the next hour, with these values providing the initial conditions for the next simulation. That strategy was not able to capture plume dynamics between hours without a large increment in computational cost or higher interpolation errors. Here, to improve the accuracy of the results and to minimise the computational cost, the adaptive technique presented by Monforte and Pérez-Foguet (2013) is used. This dynamic adaptivity scheme has been successfully applied to different transient convection-diffusion reaction models. The adaptation is driven by an error indicator which, given a solution, is used to compute the field of the mesh size needed to reduce its errors. Instead of using the gradient of the solution, as the standard error indicators used in convection-diffusion problems, Monforte and Pérez-Foguet (2013, 2014) uses the gradient of the logarithm of the solution. This makes a great difference in the simulation of air quality problems, especially near emitters where the values of the concentration can range from the order of g/m^3 close to the emitter to $\mu\text{g/m}^3$ just a few metres away. Error indicators based on the gradient of the logarithm has been successfully applied within a multimesh strategy in local scale AQM including reactions. In the multimesh approach, the evolution of each species is simulated in its own mesh. The transport step is solved independently for each species. In contrast, the reaction step is solved in a common mesh. While this mesh is the union of all meshes, there is no need to solve any system of equations based on that discretisation because reactions are uncoupled between nodes. Thus, the transport of each pollutant and the reaction of different nodes can be solved in parallel, improving the computational time of the simulation.

3 Results

In this section, we analyse and discuss the results obtained from the proposed strategy. We will compare the results from both systems between each other and with the measured data in the stations.

3.1 *WRF-ARW/AEMM/CMAQ Model*

The first step to simulate the air quality was the meteorological simulation using the WRFARW. The WRF model is configured with two nested domains with 3 km (first domain) or 1 km (second domain) of horizontal resolution. The first domain covers Catalonia, and the second domain covers the city of Barcelona and its metropolitan area (Figure 1). The results from the simulation were used to feed the CMAQ simulation. CMAQ uses the same configuration as the WRF simulation. Initial and boundary conditions for the nested domain are provided by the results of the larger domain. Meteorology-Chemistry Interface Processor (MCIP) version 4.1 is used to prepare WRF output to CMAQ model, while the AEMM model prepares emissions as required for the AERO5 and CB5 modules.

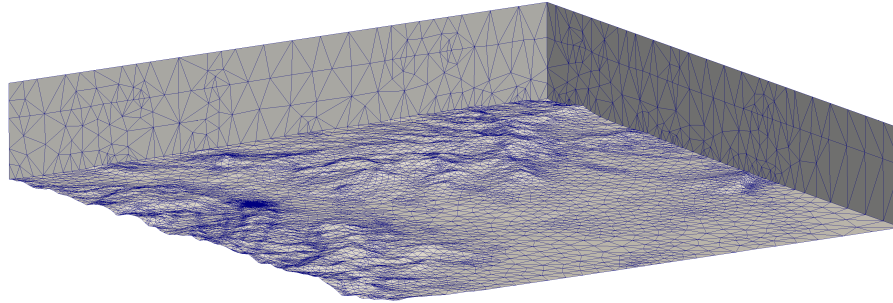
3.2 *Finite element model*

To simulate air pollution using the finite element model, we need to generate a tetrahedral mesh adapted to the terrain. The discretisation of the terrain that we used is from the shuttle radar topography mission (Farr et al., 2007); specifically, the SRTM3 version defined over an uniform grid of $3'' \times 3''$ (approximately $90 \text{ m} \times 90 \text{ m}$). Using this DTM and the mesh generation method described in Section 2.3.2, the resulting mesh has element sizes ranging from tens of centimetres to hundreds of metres. In Figure 5, a detail of the terrain discretisation and a zoom in the zone of the stack is shown, in which observed the big differences in the element sizes of the mesh. The number of elements of the mesh is 67,690 tetrahedra and 17,090 nodes.

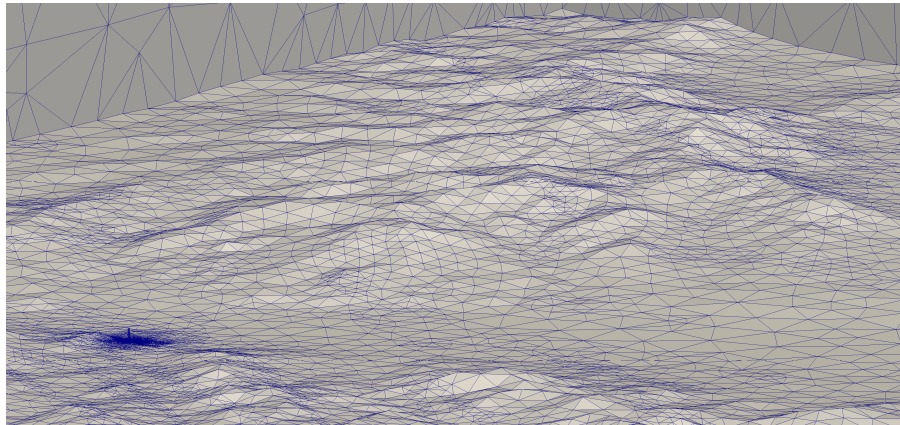
With this mesh, the wind field is simulated. The results from the WRF-ARW simulation in the inner domain are interpolated to the mesh, and incompressibility and impermeability is imposed using the mass-consistent model. Once the wind field is computed, the wind field is perturbed using the Briggs formula, and the mesh has been refined to capture the plume of the pollutants. This results in each hour having a different mesh, such that the concentration values have to be interpolated between them. Finally, pollutant transport is computed using the hourly results from the CMAQ system modelling as boundary and initial conditions for a one-way nesting. The same approach as for wind (Oliver et al., 2015) is used for interpolation of transport and reaction mesoscale data.

In this experiment, we did not consider the reaction of SO_2 , so that only pollutant transport was simulated. The time step was fixed to 15 s. The horizontal diffusion was interpolated from CMAQ, and the vertical diffusion was computed using a k-theory profile depending on the stability (Businger and Arya, 1974; Shir, 1973; Lamb and Durran, 1978). Stable boundary layer configuration is assumed during the entire simulation time.

Figure 5 Computational mesh used in the finite element simulation, (a) whole domain
(b) detail of the mesh near the stack (see online version for colours)



(a)

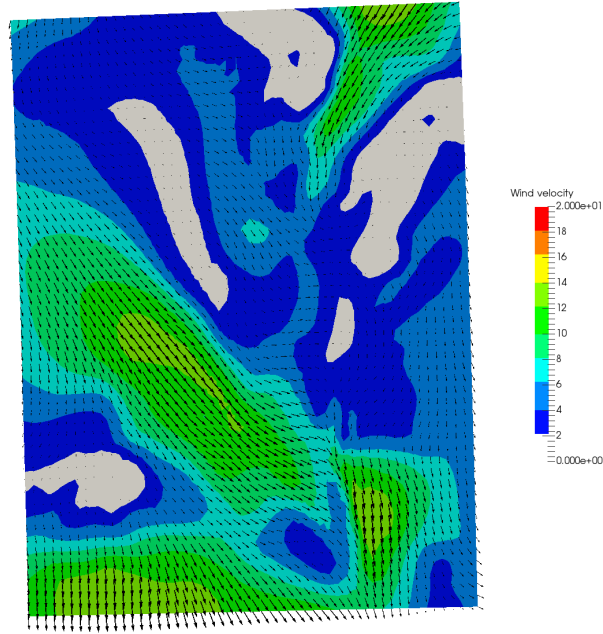


(b)

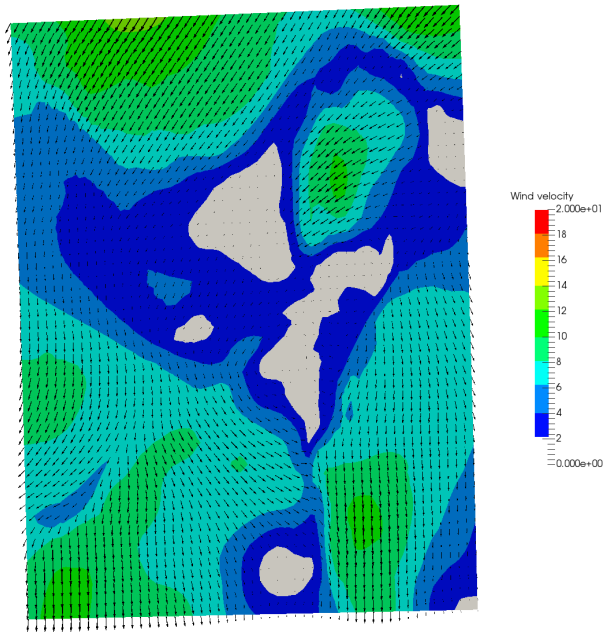
3.3 Wind field analysis

The wind field is computed using a WRF-ARW model. The time step of the simulation is set to 60 s, which is the wind field used in CMAQ. However, only hourly values are given as an output for local scale model simulations, following by default configurations of mesoscale modelling. Figure 6 shows the WRF-ARW resulting wind field used in CMAQ for hours 06:00, 12:00, 18:00, and 24:00. Values at 10 m above ground level are shown to compare wind distributions. We can observe that the wind velocities at 06:00 and 12:00 are low, and that they increase at 18:00, with a peak at 00:00 of the next day. The main direction of the wind field during the entire day was from north-west to south-east. We also want to note that, in the zone of the emitter, the wind velocities were not especially high (between 4 m/s and 10 m/s). This low velocity can explain the high concentrations on this day near the emitter. Looking at the wind direction, we can anticipate that the most affected areas near the emitter will be to the east and the south.

Figure 6 CMAQ wind field at 10 m above ground level, (a) 06:00 (b) 12:00 (c) 18:00 (d) 00:00 (see online version for colours)

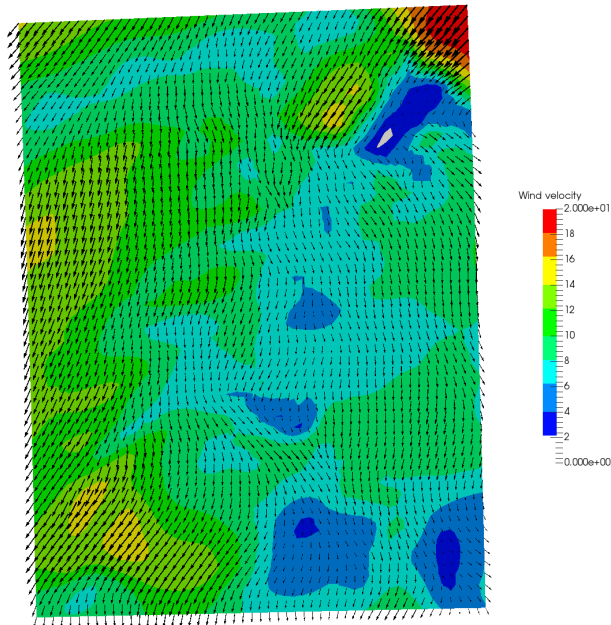


(a)

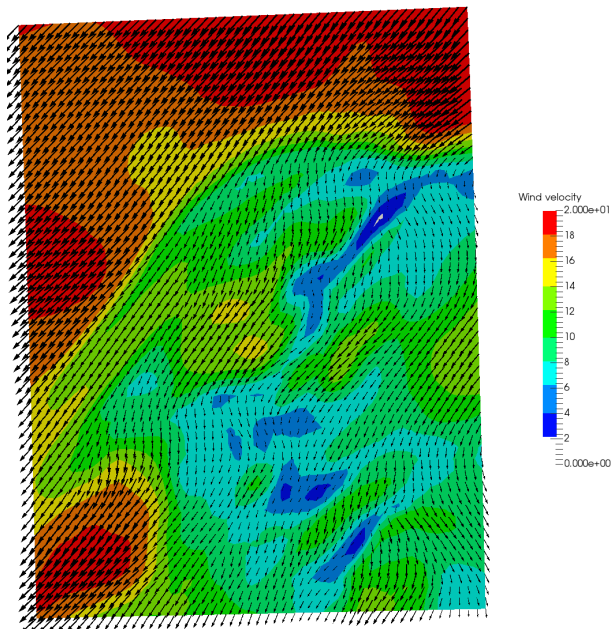


(b)

Figure 6 CMAQ wind field at 10 m above ground level, (a) 06:00 (b) 12:00 (c) 18:00 (d) 00:00 (continued) (see online version for colours)

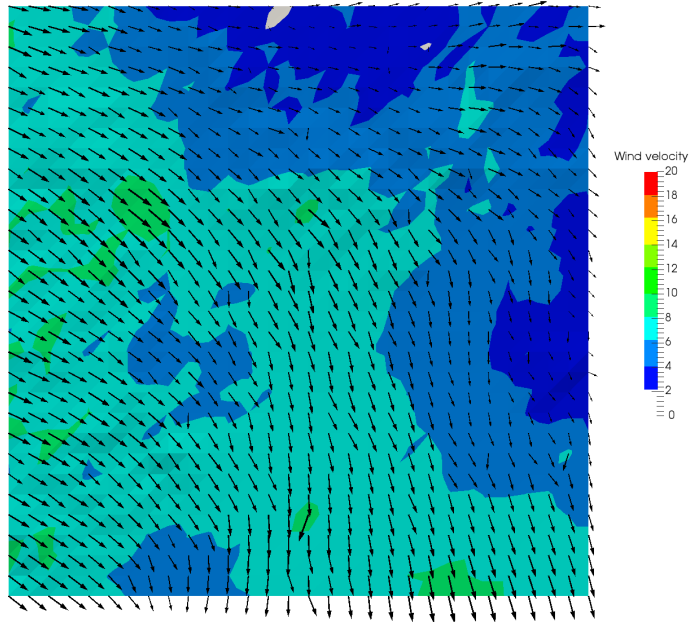


(c)

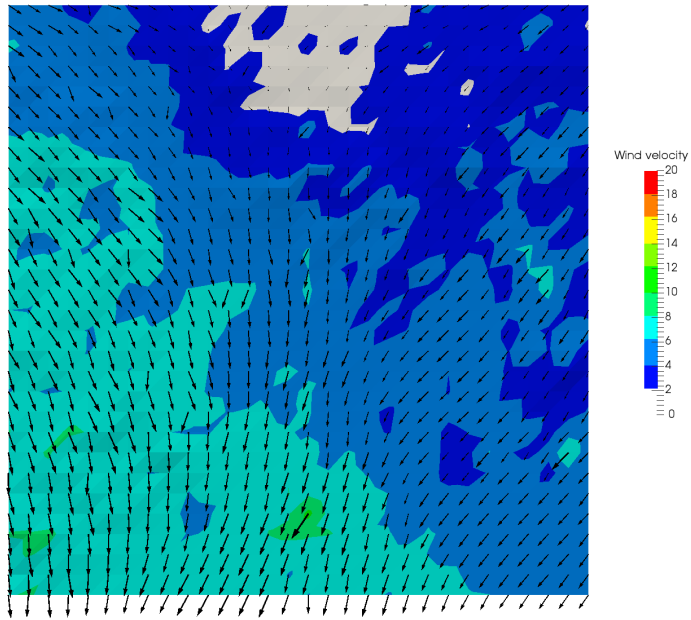


(d)

Figure 7 FEM wind field at 10 m above ground level, (a) 06:00 (b) 12:00 (c) 18:00 (d) 00:00 (see online version for colours)

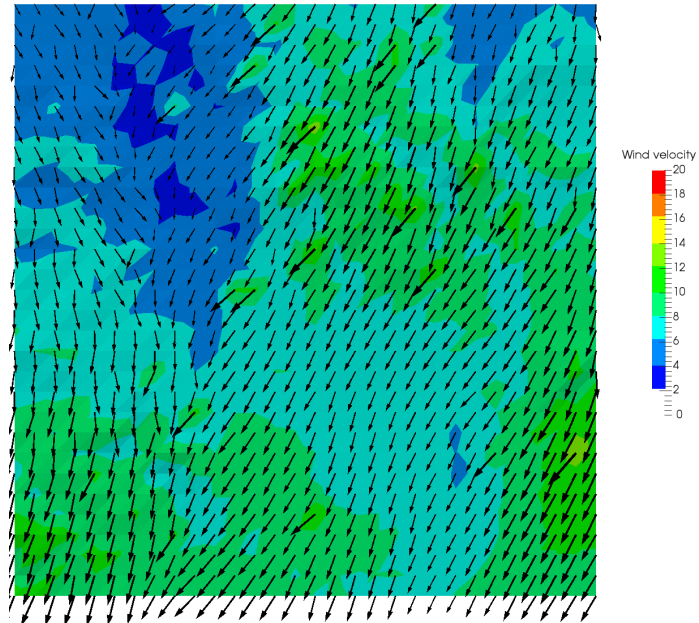


(a)

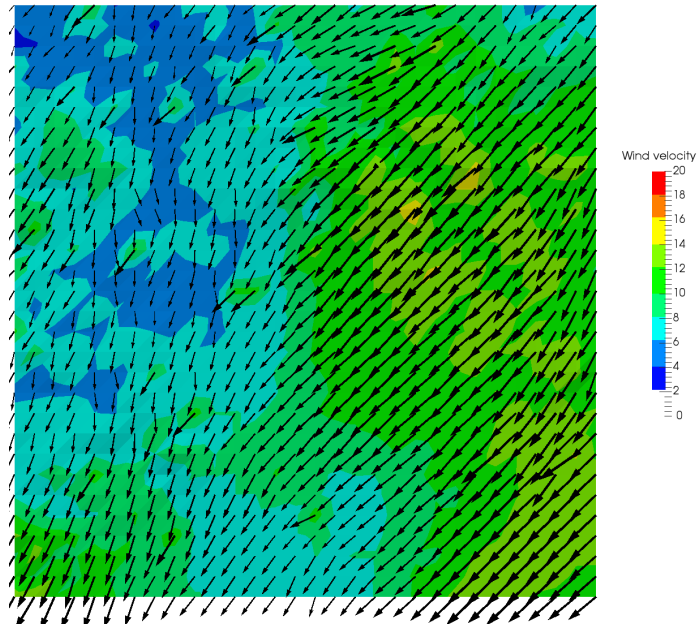


(b)

Figure 7 FEM wind field at 10 m above ground level, (a) 06:00 (b) 12:00 (c) 18:00 (d) 00:00 (continued) (see online version for colours)



(c)



(d)

Figure 7 represents the values of the wind field that will be used in the local scale simulation. We can observe that the main direction and velocity of the wind field is similar to the WRF-ARW but that some differences arise. For example, the velocities are constantly slower, with differences in the wind direction, probably due to the better representation of the terrain in the local scale mesh.

3.4 Pollution analysis

At this point, we can analyse the concentration of SO_2 . We will examine the values of both the maximum of one-hour and the daily levels in the measurement stations. We will also compare the CMAQ and FEM simulations. The comparison will be carried out in two stations: one near the station (Alaba) and the other far from it (Viladecans).

First, we examine the max-1h and daily levels of SO_2 for both simulations. Figures 8 and 9 represent, respectively, the maximum value achieved at the one-hour distributions and the daily mean concentration. Qualitatively, we can observe that in the CMAQ results, the emitter is not the largest contributor in the domain, while in the micro-scale results, all of the pollutant concentration comes from the emitter and the boundary conditions, with the emitter the larger contributor. For a more quantitative analysis, the maximum levels at one-hour and daily are listed in Table 2.

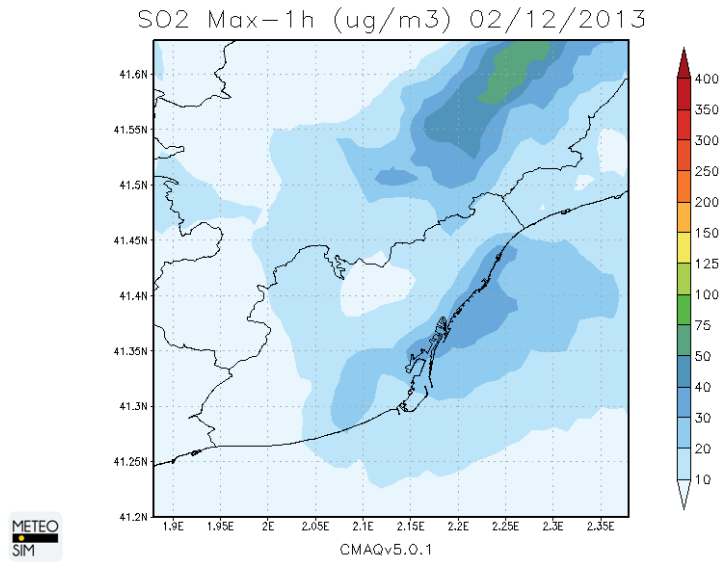
Table 2 Comparison of max-1h and daily concentrations for all the stations using CMAQ, FEM, and the measured data

Station	Max-1h conc. ($\mu\text{g}/\text{m}^3$)			Daily conc. ($\mu\text{g}/\text{m}^3$)		
	Measured	FEM	CMAQ	Measured	FEM	CMAQ
Alaba	96	74	7.8	25	19	3.3
Ribot	4.0	9.9	13	1.5	1.6	4.5
Pallejà	15	87	8.2	8.2	15	4.8
Gavà	4.0	0.007	4.9	3.2	0.002	2.5
Viladecans	3.0	0.02	5.3	2.2	0.002	3.2
St. Feliu	7.0	0.1	10	4.6	0.01	4.4
Prat CEM	4.0	0.07	13	2.4	0.01	5.7
Prat PAU	6.0	0.2	15	3.1	0.03	6.2
Vall d'Hebron	3.0	0.4	8.2	1.6	0.1	4.8
Gracia	16	0.5	8.6	6.3	0.2	4.6
Eixample	2.0	0.9	11	1.1	0.2	6.1
Palau Reial	1.0	0.1	7.4	1.0	0.03	4.6

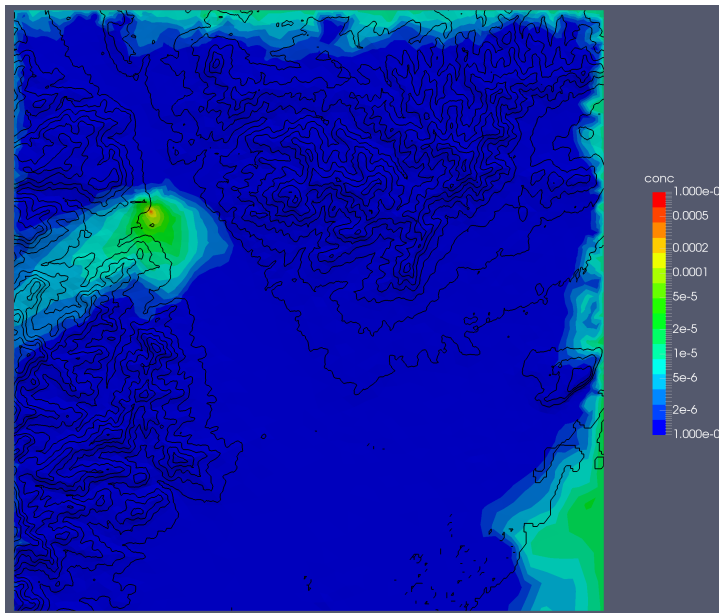
The first two stations on the table are the nearest stations downstream to the emitter, and therefore those more influenced by the SO_2 emission, especially the Alaba station, with the highest maximum one-hour and daily concentrations. If we compare the results from the finite element simulation and the CMAQ system simulation, we can observe that the values from CMAQ are much lower in the Alaba station than those measured. The finite element results are more in agreement with the measured data, although it also underpredicts. In the Ribot station, the results from the finite element simulation are closer to the measured data, especially in the daily levels, but the simulated levels are higher than the measured ones for both daily and max-1h levels. The CMAQ system does

not recover the measured data, and its values are greater than both the measured and the simulated with the FEM.

Figure 8 Max 1 h concentration on day 02/12/2013 (see online version for colours)



(a)



(b)

Figure 9 Daily concentration on day 02/12/2013, (a) CMAQ system simulation (b) FEM simulation (see online version for colours)

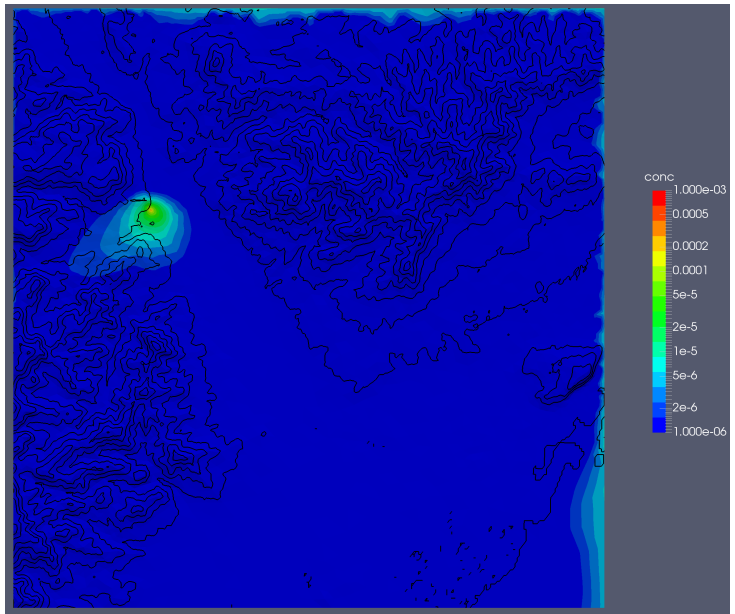
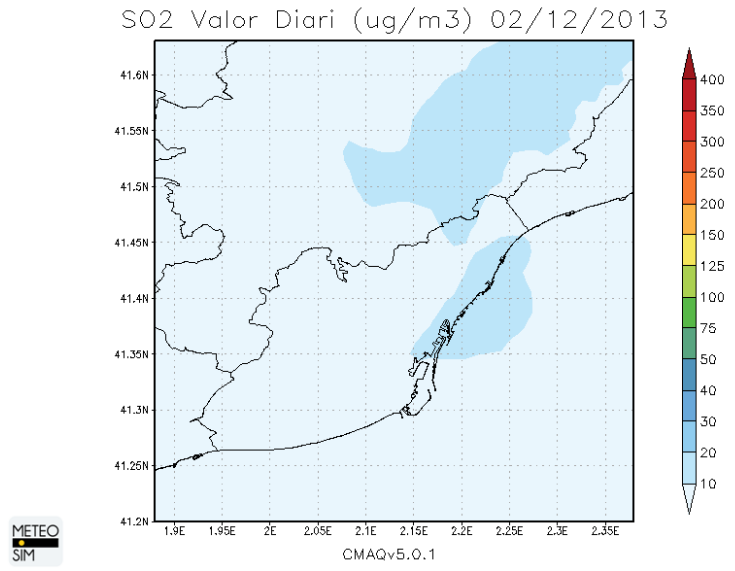


Figure 10 Isosurfaces pollutant concentrations (see online version for colours)

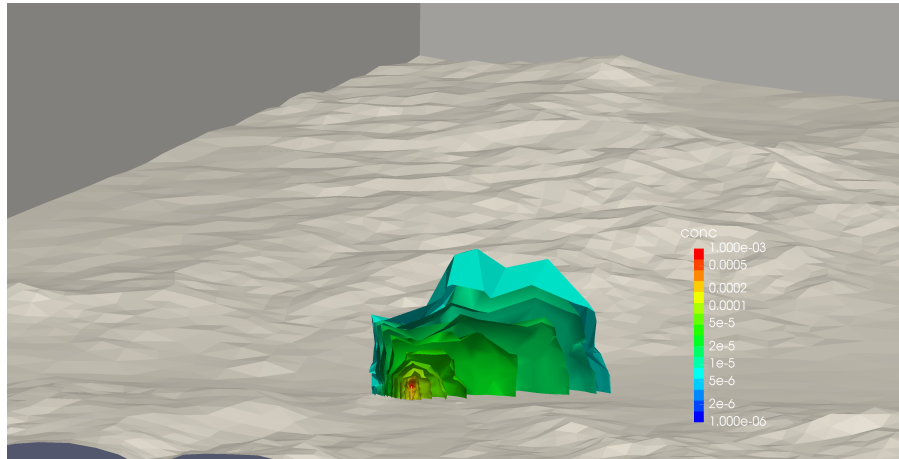
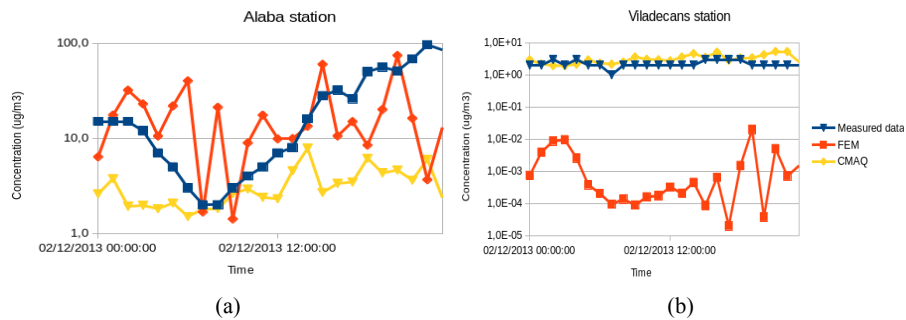


Figure 11 Comparison of simulated concentrations versus those observed for (a) a station close to the emitter (Alaba station) and (b) a more distant station (Viladecans station) (see online version for colours)



The next station, Pallejà, is close to the emitter but upstream. In this case, neither the CMAQ simulation nor the finite element model reproduces the measurements accurately. For the CMAQ simulation, the result levels are lower than half of the measured ones. On the other hand, the values of the FEM are much larger, especially maximum values; the daily mean is only doubled. These large values can result from relatively high values of horizontal diffusion with respect to wind velocity. Figure 10 shows a transversal slice of the resulting pollutant plume of the finite element solution. The different isosurfaces are displayed; we can observe upstream concentrations. The rest of the stations are distant to the emitter, and all have the same pattern: the FEM values are near zero, the only emissions are from the emitter, and CMAQ results are in the same order of magnitude as the measured ones.

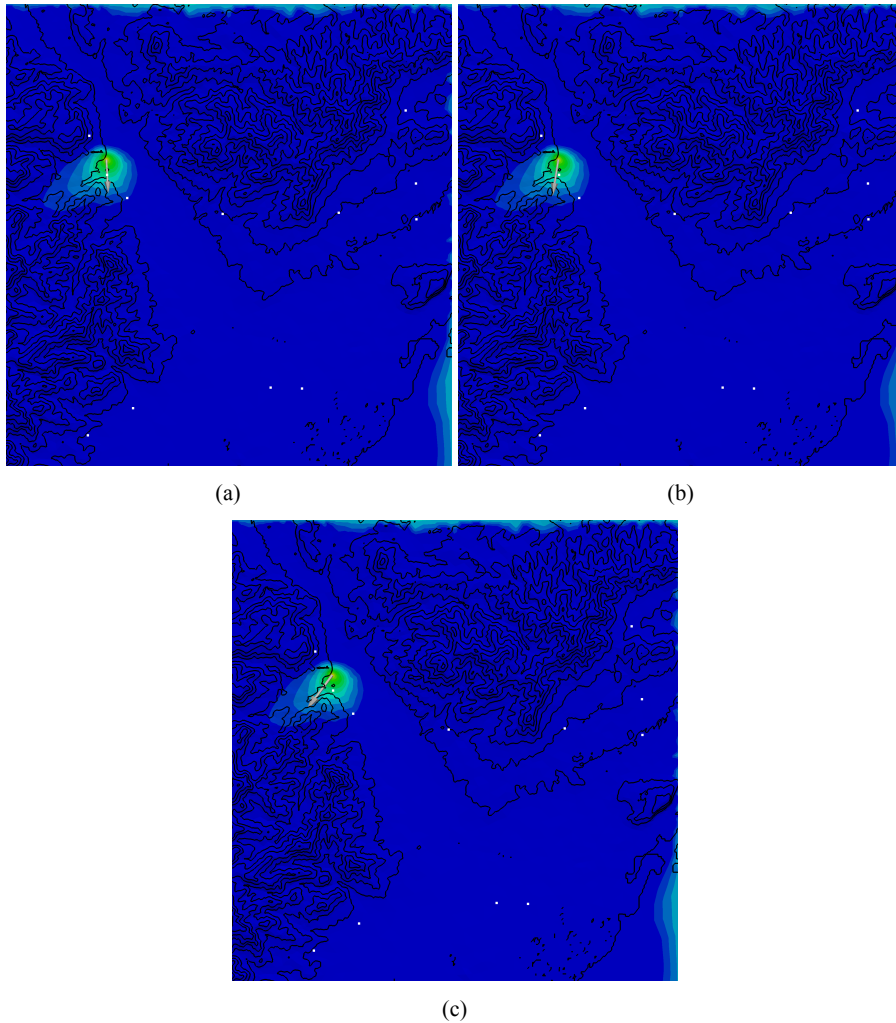
Table 3 Simulated and measured concentrations ($\mu\text{g}/\text{m}^3$) at a near station (Alaba) and a distant station (Viladecans)

<i>Hour</i>	<i>Alaba station</i>			<i>Viladecans station</i>		
	<i>Measured</i>	<i>FEM</i>	<i>CMAQ</i>	<i>Measured</i>	<i>FEM</i>	<i>CMAQ</i>
00:00	15	6.4	2.6	2	7.4E-04	2.9
01:00	15	17.5	3.8	2	3.9E-03	2.2
02:00	15	32.0	1.9	3	8.7E-03	1.9
03:00	12	23.0	2.0	2	9.6E-03	1.9
04:00	7	10.6	1.8	3	2.6E-03	2.1
05:00	5	21.9	2.1	2	3.8E-04	2.9
06:00	3	40.1	1.5	2	2.0E-04	2.3
07:00	2	1.7	1.8	1	9.4E-05	2.1
08:00	2	21.2	1.8	2	1.4E-04	2.5
09:00	3	1.4	2.6	2	8.9E-05	3.6
10:00	4	8.9	2.9	2	1.6E-04	3.0
11:00	5	17.5	2.4	2	1.7E-04	2.9
12:00	7	9.9	2.3	2	3.2E-04	2.7
13:00	8	9.9	4.6	2	2.1E-04	3.6
14:00	16	13.4	7.8	2	4.5E-04	4.6
15:00	28	59.8	2.7	3	8.6E-05	3.5
16:00	32	10.6	3.3	3	6.4E-04	5.1
17:00	26	15.0	3.5	3	2.0E-05	2.8
18:00	50	8.5	6.2	3	1.5E-03	3.3
19:00	56	20.1	4.3	2	2.0E-02	3.4
20:00	51	74.3	4.6	2	3.7E-05	4.2
21:00	68	16.2	3.6	2	5.0E-03	5.3
22:00	96	3.7	6.0	2	7.1E-04	5.3
23:00	85	13.0	2.4	2	1.5E-03	2.5

Based on the results from the maximum one-hour and daily concentrations, we decided to carry out a more careful analysis in the Alaba and Viladecans stations. Figure 11 shows the concentration during the day in both stations, and Table 3 lists the concentrations. We can observe that the results from the Viladecans station are as expected: the results from CMAQ are very close to the measured ones, and the finite element simulation concentrations are near zero, since the emitter does not affect this station. The case of the Alaba station is more interesting. The CMAQ simulation underpredicts the observed data, it is not far but is not able to capture the cycle of the immission levels. The FEM results are closer to the measured data, but the concentration is a zigzag line that surrounds the measured data, so the results are not really good. One of the causes of these big swings in the concentration can be the resolution of the wind field. The concentrations in Table 3 reveal a large swing from 40.1 and 1.7 between 06:00 and 07:00 $\mu\text{g}/\text{m}^3$. In Figure 12, we compare the wind direction and velocity in the top of the stack from 5:00 to 7:00. We can see how the wind field in these three hours turns from east to south-east. At 05:00, the

wind direction points directly towards the Alaba station, and this direction is maintained in the FEM simulation during the whole hour. This direction can explain why the concentration measurement of this hour is so high. We assume that the direction between 5:00 and 6:00 turned slowly, moving away from the station, and thus giving a lower concentration. During the next hour (from 6:00 to 7:00), the wind field turns further south, giving a smaller concentration at 7:00. This observation is in agreement with the values of the concentration at the Alaba station during this time frame, and we can assume that if the wind field resolution had been higher, the concentration results would have been better.

Figure 12 Wind vector at the top of the stack for hours (a) 05:00, (b) 06:00 and (c) 07:00
(see online version for colours)



Note: Locations of stations are also displayed.

3.5 Computational time

Finally, we will analyse the computational time required to solve the FEM. The computational time is one of the main issues with the FEM because the adapted mesh asks for a large number of elements; remember that near the emitter, the elements are only a few centimetres. The simulated period was 49 hours long, with a time-step of 15 s. As the problem only involved the pollutant transport, no reactions were considered. With this configuration, the total CPU time was 26 hours and 45 minutes, so the simulation time is a little bit more than half of the simulated time. We should note that, due to the adaptation phase, some simulated hours are recomputed to use the new refined mesh.

4 Conclusions

This work presents a novel system to simulate the air quality near large emitters. The main idea of the presented approach is to simulate the transport and reaction of pollutants with the highest possible resolution while minimising computational costs. To this end, we combine a nested grid approach and a dynamically adaptive finite element model. The nested grid system consists of the mesoscale meteorological model WRF-ARW, the AEMM, and the air quality model CMAQ. This system uses a nested set of grids with a lower-end resolution of 1 km. The finite element model uses a tetrahedral mesh adapted to the terrain and to the evolution of the concentrations, which greatly improves the spatial resolution using elements with sizes ranging from kilometres to centimetres. This high resolution can improve the accuracy of the model, although it also implies more computational time for resolving the model.

In this article, we applied the proposed approach to simulate the immission levels around a large emitter in the surroundings of Barcelona. This emitter is an important contributor of SO₂ from an industrial plant. The episode that we chose corresponds to a day during which the concentration of SO₂ was higher than average. Results were analysed and validated by comparing them against measurement data from the Air Quality Network of the Catalan Government. From all the measurement stations, three are close to the emitter and largely affected by it, and the rest are further and affected by other sources.

The methodology of this approach is to simulate first the air quality using the WRFARW/AEMM/CMAQ coupled system, and then to interpolate the solution into the finite element mesh, using the coupled system results for the initial and boundary conditions. The WRF-ARW/AEMM/CMAQ system takes into account all the emissions of the domain, while the finite element model just takes into account the emissions of the large emitter, and the emissions that come from the boundaries. It is important to note that the presented approach is one-way, and that the results from the finite element model are not used in the mesoscale model.

We analysed the results by comparing those from the WRF-ARW/AEMM/CMAQ system with those from the finite element model. First, the daily and maximum one-hour concentration levels were compared in all the measurement stations. In the two stations located downstream to the emitter, the finite element model presents much better results than the coupled system. In the stations further away, the coupled system captures these levels correctly, and the results from the FEM are almost zero because no emissions are taken into account. The results in the station located upstream to the emitter (Pallejà)

need to be considered more carefully. In this station, the results from the finite element model overpredict the measured data. This overprediction can be explained by the relatively high horizontal diffusion values, which need to be analysed further to clarify the influence of CMAQ diffusion values and numerical diffusion introduced during finite element model simulations.

A more detailed analysis was carried out in two characteristic stations: Alaba station (closer, downstream), and Viladecans (more distant). In the Viladecans station, the results were as expected: the coupled system captures the measured results, and the finite element model concentrations are near zero. The results from the Alaba station show that the coupled system underpredicts the solution, but that the finite element results are close to the measured data and follow its shape. However, the solutions show large swings that are related with the time resolution of the wind field (the wind field is updated from the mesoscale model every hour). As the mesoscale model already computes time integration with a shorter time step, of one minute, further analyses can be done to determine the optimal time step for local model computation. We would like to point out that an increased time resolution will likely increase the required computational time, as it involves more frequent updates for the wind and plume rise modelling.

Overall, we can conclude that the proposed method improves the solution from the nested grid technique alone, especially near the emitter, where its results are closer to those observed. Still, further developments are required in the finite element model, especially regarding the influence of horizontal diffusion on the outputs of interest and the influence of the wind field temporal resolution, while keeping the computational cost within affordable limits. Further improvements are also needed in relation with the computational time; in its current form, the proposed approach is not suitable for an operational model. However, it can be used as a diagnostic model or even for forecasting punctual episodes, like those presented here. Finally, we want to remark that, in future work, it would be interesting to carry out a comparative analysis with other subgrid scale methods, as well as to use the finite element local model, to analyse the variability of the concentration in a hybrid model.

Acknowledgements

This work has been supported by the Spanish Government ('Ministerio de Economía, Industria y Competitividad') and FEDER: grant contract CTM2014-55014-C3-1-R; the Spanish National Programme for Recruitment and Incorporation of Human Resources: PTQ-12-05244; and the Catalan Government ('Agència de Gestió d'Ajuts Universitaris i de Recerca (AGAUR)'): 'Engineering Sciences and Global Development' project, ref. 2014SGR1545:2014-2016. The authors gratefully acknowledge the Catalan Government for providing the industrial emissions inventory and the measured pollution data from its Air Quality Network.

References

- Albani, R.A., Duda, F.P. and Pimentel, L.C.G. (2015) 'On the modeling of atmospheric pollutant dispersion during a diurnal cycle: a finite element study', *Atmospheric Environment*, Vol. 118, pp.19–27.
- Arasa, R., Domingo-Dalmau, A. and Vargas, R. (2016a) 'Using a coupled air quality modeling system for the development of an air quality plan in Madrid (Spain): source apportionment and analysis evaluation of mitigation measures', *Journal of Geoscience and Environment Protection*, Vol. 4, No. 3, pp.46–61.
- Arasa, R., Porras, I., Domingo-Dalmau, A., Picanyol, M., Codina, B., González, M.Á. and Piñón, J. (2016b) 'Defining a standard methodology to obtain optimum WRF configuration for operational forecast: application over the Port of Huelva (Southern Spain)', *Atmospheric and Climate Sciences*, Vol. 6, No. 2, pp.329–350.
- Arasa, R., Lozano-García, A. and Codina, B. (2014) 'Evaluating mitigation plans over traffic sector to improve NO₂ levels in Andalusia (Spain) using a regional-local scale photochemical modelling system', *Open Journal of Air Pollution*, Vol. 3, No. 3, pp.70–86.
- Arasa, R., Picanyol, M. and Solé, J. (2013) 'Analysis of the integrated environmental and meteorological forecasting and alert system (SIAM) for air quality applications over different regions of the Iberian Peninsula', in *Proceedings from the 15th International Conference on Harmonisation within Atmospheric Dispersion Modelling for Regulatory Purposes*, Madrid.
- Businger, J.A. and Arya, S. (1974) 'The height of the mixed layer in the stably stratified planetary boundary layer', *Advances in Geophysics*, Vol. 18, No. A, pp.73–92.
- Byun, D. and Schere, K.L. (2006) 'Review of the governing equations, computational algorithms, and other components of the models-3 community multiscale air quality (CMAQ) modeling system', *Applied Mechanics Reviews*, Vol. 59, No. 2, pp.51–77.
- Carlton, A.G., Bhawe, P.V., Napelenok, S.L., Edney, E.O., Sarwar, G., Pinder, R.W., Pouliot, G.A. and Houyoux, M. (2010) 'Model representation of secondary organic aerosol in CMAQv4.7', *Environmental Science & Technology*, Vol. 44, No. 22, pp.8553–8560.
- Cavellin, L.D., Weichenthal, S., Tack, R., Ragetti, M.S., Smargiassi, A. and Hatzopoulou, M. (2016) 'Investigating the use of portable air pollution sensors to capture the spatial variability of traffic-related air pollution', *Environmental Science & Technology*, Vol. 50, No. 1, pp.313–320.
- Ching, J. and Majeed, M.A. (2012) 'An approach to characterize within-grid concentration variability in air quality models', *Atmospheric Environment*, Vol. 49, pp.348–360.
- Chowdhury, B., Karamchandani, P., Sykes, R., Henn, D. and Knipping, E. (2015) 'Reactive puff model SCICHEM: model enhancements and performance studies', *Atmospheric Environment*, Vol. 117, pp.242–258.
- European Environment Agency (EEA) (2007) *Air Pollution in Europe 1990–2004*, Technical Report EEA-2/2007.
- Farr, T.G., Rosen, P.A., Caro, E., Crippen, R., Duren, R., Hensley, S., Kobrick, M., Paller, M., Rodriguez, E., Roth, L., Seal, D., Shaffer, S., Shimada, J., Umland, J., Werner, M., Oskin, M., Burbank, D. and Alsdorf, D. (2007) 'The shuttle radar topography mission', *Reviews of Geophysics*, Vol. 45, No. 2.
- Gao, M., Carmichael, G.R., Wang, Y., Saide, P.E., Yu, M., Xin, J., Liu, Z. and Wang, Z. (2016) 'Modeling study of the 2010 regional haze event in the north china plain', *Atmospheric Chemistry and Physics*, Vol. 16, No. 3, pp.1673–1691.
- Grell, G.A., Peckham, S.E., Schmitz, R., McKeen, S.A., Frost, G., Skamarock, W.C. and Eder, B. (2005) 'Fully coupled 'online' chemistry within the WRF model', *Atmospheric Environment*, Vol. 39, No. 37, pp.6957–6975.
- Gressent, A., Sauvage, B., Cariolle, D., Evans, M., Leriche, M., Mari, C. and Thouret, V. (2016) 'Modeling lightning-NO_x chemistry on a sub-grid scale in a global chemical transport model', *Atmospheric Chemistry and Physics*, Vol. 16, No. 9, pp.5867–5889.

Simulating large emitters using CMAQ and a local scale finite element model 27

- Isakov, V., Irwin, J.S. and Ching, J. (2007) 'Using CMAQ for exposure modeling and characterizing the subgrid variability for exposure estimates', *Journal of Applied Meteorology and Climatology*, Vol. 46, No. 9, pp.1354–1371.
- Isakov, V., Touma, J.S., Burke, J., Lobdell, D.T., Palma, T., Rosenbaum, A. and Ozkaynak, H. (2009) 'Combining regional- and local-scale air quality models with exposure models for use in environmental health studies', *Journal of the Air & Waste Management Association*, Vol. 59, No. 4, pp.461–472.
- Jiang, B. (1998) *The Least-Squares Finite Element Method*, Springer, Berlin, Heidelberg.
- Karamchandani, P., Johnson, J., Yarwood, G. and Knipping, E. (2014) 'Implementation and application of sub-grid-scale plume treatment in the latest version of EPA's third generation air quality model, CMAQ 5.01', *Journal of the Air & Waste Management Association*, Vol. 64, No. 4, pp.453–467.
- Karamchandani, P., Lohman, K. and Seigneur, C. (2008) 'Using a sub-grid scale modeling approach to simulate the transport and fate of toxic air pollutants', *Environmental Fluid Mechanics*, Vol. 9, No. 1, pp.59–71.
- Karamchandani, P., Santos, L., Sykes, I., Zhang, Y., Tonne, C. and Seigneur, C. (2000) 'Development and evaluation of a state-of-the-science reactive plume model', *Environmental Science & Technology*, Vol. 34, No. 5, pp.870–880.
- Karamchandani, P., Seigneur, C., Vijayaraghavan, K. and Wu, S-Y. (2002) 'Development and application of a state-of-the-science plume-in-grid model', *Journal of Geophysical Research*, Vol. 107, No. D19, pp.ACH 12-1–ACH 12-13.
- Karamchandani, P., Vijayaraghavan, K. and Yarwood, G. (2011) 'Sub-grid scale plume modeling', *Atmosphere*, Vol. 2, No. 4, pp.389–406.
- Karamchandani, P., Zhang, Y. and Chen, S-Y. (2012) 'Development and initial application of a sub-grid scale plume treatment in a state-of-the-art online multi-scale air quality and weather prediction model', *Atmospheric Environment*, Vol. 63, pp.125–134.
- Kim, Y., Seigneur, C. and Duclaux, O. (2014) 'Development of a plume-in-grid model for industrial point and volume sources: application to power plant and refinery sources in the Paris region', *Geoscientific Model Development*, Vol. 7, No. 2, pp.569–585.
- Lamb, R.G. and Durran, D.R. (1978) 'Eddy diffusivities derived from a numerical model of the convective planetary boundary layer', *Il Nuovo Cimento C*, Vol. 1, No. 1, pp.1–17.
- Lee, C.K. (2001) 'On curvature element-size control in metric surface mesh generation', *International Journal for Numerical Methods in Engineering*, Vol. 50, No. 4, pp.787–807.
- Lin, C-J. and Moré, J.J. (1999) 'Incomplete Cholesky factorizations with limited memory', *SIAM Journal on Scientific Computing*, Vol. 21, No. 1, pp.24–45.
- Liu, C-H. and Leung, D.Y.C. (2005) 'Finite element solution to passive scalar transport behind line sources under neutral and unstable stratification', *International Journal for Numerical Methods in Fluids*, Vol. 50, No. 5, pp.623–648.
- Marshall, J.D., Nethery, E. and Brauer, M. (2008) 'Within-urban variability in ambient air pollution: comparison of estimation methods', *Atmospheric Environment*, Vol. 42, No. 6, pp.1359–1369.
- Monforte, L. and Pérez-Foguet, A. (2013) 'A multimesh adaptive scheme for air quality modeling with the finite element method', *International Journal for Numerical Methods in Fluids*, Vol. 74, No. 6, pp.387–405.
- Monforte, L. and Pérez-Foguet, A. (2014) 'Esquema adaptativo para problemas tridimensionales de convección-difusión', *Revista Internacional de Métodos Numéricos para Cálculo y Diseño en Ingeniería*, Vol. 30, No. 1, pp.60–67.
- Montenegro, R., Oliver, A., Rodríguez, E., Escobar, J.M., Montero, G. and Pérez-Foguet, A. (2012) 'Three-dimensional finite element modelling of stack pollutant emissions', in *Proceedings of the Eighth International Conference on Engineering Computational Technology*, Civil-Comp, Ltd.

- Oliver, A., Montero, G., Montenegro, R., Rodríguez, E., Escobar, J.M. and Pérez-Foguet, A. (2012) 'Finite element simulation of a local scale air quality model over complex terrain', *Advances in Science and Research*, Vol. 8, No. 1, pp.105–113.
- Oliver, A., Montero, G., Montenegro, R., Rodríguez, E., Escobar, J.M. and Pérez-Foguet, A. (2013) 'Adaptive finite element simulation of stack pollutant emissions over complex terrains', *Energy*, Vol. 49, pp.47–60.
- Oliver, A., Rodríguez, E., Escobar, J.M., Montero, G., Hortal, M., Calvo, J., Cascón, J.M. and Montenegro, R. (2015) 'Wind forecasting based on the HARMONIE model and adaptive finite elements', *Pure and Applied Geophysics*, Vol. 172, No. 1, pp.109–120.
- Pérez-Foguet, A. and Oliver, A. (2009) 'Coupling mesoscale air quality models with finite element computation of dispersion at local level', in *European Geosciences Union General Assembly 2009*, Geophysical Research Abstracts.
- Pérez-Foguet, A., Oliver, A., Escobar, J.M. and Rodríguez, E. (2006) 'Finite element simulation of chimney emissions: a proposal for near field impact assessment in highly complex terrains', in *Proceedings of the Fifth International Conference on Engineering Computational Technology*, Civil-Comp, Ltd.
- Qin, M., Wang, X., Hu, Y., Huang, X., He, L., Zhong, L., Song, Y., Hu, M. and Zhang, Y. (2015) 'Formation of particulate sulfate and nitrate over the pearl river delta in the fall: diagnostic analysis using the community multiscale air quality model', *Atmospheric Environment*, Vol. 112, pp.81–89.
- Raffort, V., Kim, Y., Donnat, L., Juery, C., Seigneur, C. and Duclaux, O. (2015) 'Plume-in-grid model for the evaluation of particulate matter contribution of industrial point and volume sources: application to refinery sources in the Paris region', *International Journal of Environment and Pollution*, Vol. 57, Nos. 3/4, p.238.
- Rissman, J., Arunachalam, S., Woody, M., West, J.J., BenDor, T. and Binkowski, F.S. (2013) 'A plume-in-grid approach to characterize air quality impacts of aircraft emissions at the Hartsfield-Jackson Atlanta International Airport', *Atmospheric Chemistry and Physics*, Vol. 13, No. 18, pp.9285–9302.
- Rodríguez-Ferran, A. and Sandoval, M. (2007) 'Numerical performance of incomplete factorizations for 3D transient convection-diffusion problems', *Advances in Engineering Software*, Vol. 38, No. 6, pp.439–450.
- Ropp, D.L., Shadid, J.N. and Ober, C.C. (2004) 'Studies of the accuracy of time integration methods for reaction-diffusion equations', *Journal of Computational Physics*, Vol. 194, No. 2, pp.544–574.
- Rosenbaum A. (2005) *The HAPEM5 User's Guide: Hazardous Air Pollutant Exposure Model, Version 5*, USEPA [online] https://www.epa.gov/sites/production/files/2013-08/documents/hapem5_guide.pdf.
- Saha, S., Moorthi, S., Wu, X., Wang, J., Nadiga, S., Tripp, P., Behringer, D., Hou, Y-T., Chuang, H., Iredell, M., Ek, M., Meng, J., Yang, R., Mendez, M.P., van den Dool, H., Zhang, Q., Wang, W., Chen, M. and Becker, E. (2014) 'The NCEP climate forecast system version 2', *Journal of Climate*, Vol. 27, No. 6, pp.2185–2208.
- Sarrate, J. and Huerta, A. (2000) 'Efficient unstructured quadrilateral mesh generation', *International Journal for Numerical Methods in Engineering*, Vol. 49, No. 10, pp.1327–1350.
- Sarrate, J. and Huerta, A. (2001) 'An improved algorithm to smooth graded quadrilateral meshes preserving the prescribed element size', *Communications in Numerical Methods in Engineering*, Vol. 17, No. 2, pp.89–99.
- Shir, C. (1973) 'A preliminary numerical study of atmospheric turbulent flows in the idealized planetary boundary layer', *Journal of the Atmospheric Sciences*, Vol. 30, No. 7, pp.1327–1339.
- Si, H. (2015) 'TetGen, a Delaunay-based quality tetrahedral mesh generator', *ACM Transactions on Mathematical Software*, Vol. 41, No. 2, pp.1–36.

Simulating large emitters using CMAQ and a local scale finite element model 29

- Skamarock, W.C. and Klemp, J.B. (2008) 'A time-split nonhydrostatic atmospheric model for weather research and forecasting applications', *Journal of Computational Physics*, Vol. 227, No. 7, pp.3465–3485.
- Skamarock, W.C., Klemp, J.B., Dudhia, J., Gill, D.O., Barker, D.M., Duda, M.G., Huang, X-Y., Wang, W. and Powers, J.G. (2008) *A Description of the Advanced Research WRF Version 3*, Technical Report NCAR/TN-475+STR, National Center for Atmospheric Research.
- Sokhi, R., José, R.S., Kitwiroon, N., Fragkou, E., Pérez, J. and Middleton, D. (2006) 'Prediction of ozone levels in London using the MM5-CMAQ modelling system', *Environmental Modelling & Software*, Vol. 21, No. 4, pp.566–576.
- van der Swaluw, E., Kranenburg, R., de Vries, W., Sauter, F., Kruit, R.W., Aben, J., Manders, A., Velders, G., Schaap, M. and van Pul, A. (2016) 'LEO: combination of a plume and grid model in the Netherlands', in *Springer Proceedings in Complexity*, Springer Science, pp.307–311.
- Wałaszek, K., Kryza, M. and Werner, M. (2015) 'Application of chemical dispersion model during a high ozone episode in south-west Poland', *International Journal of Environment and Pollution*, Vol. 58, Nos. 1/2, p.124.
- Yarwood, G., Rao, S., Yocke, M. and Whitten, G. Z. (2005) *Updates to the Carbon Bond Chemical Mechanism: CB05*, Technical Report RT-040-0675, Final Report to the US EPA.
- Žabkar, R., Honzak, L., Skok, G., Forkel, R., Rakovec, J., Cegljar, A. and Žagar, N. (2015) 'Evaluation of the high resolution WRF-chem (v3.4.1) air quality forecast and its comparison with statistical ozone predictions', *Geoscientific Model Development*, Vol. 8, No. 7, pp.2119–2137.